JOM, Vol. 73, No. 4, 2021
https://doi.org/10.1007/s11837-020-04464-2

The Characteristics of the Phase Transition of Air-Quenched Ladle Furnace Slag

JIHUI ZHAO,[1,2] YIREN WANG,[1,5] KUIZHEN FANG,[3] YE ZHENG,[4] and DONGMIN WANG[3]

1.—School of Civil Engineering, Sun Yat-Sen University, Guangzhou, China. 2.—Southern Marine Science and Engineering Guangdong Laboratory, Zhuhai, China. 3.—School of Chemical and Environmental Engineering, China University of Mining and Technology, Beijing, China. 4.—Department of Civil Engineering, McGill University, Montreal, Canada. 5.—e-mail: wangyr55@mail.sysu.edu.cn

The application of ladle furnace slag (LFS) as a cementitious material is limited due to its low cementitious activity and volume stability. This study incorporated air quenching to optimize the crystalline states and types of LFS, and investigated the characteristics of phase transition considering apparent morphology and mineral compositions. Compared to slow-cooled LFS, air-quenched LFS mainly comprises spherical vitreous particles with loose porous structures, ranging from 0.5 mm to 10 mm. Its mineral composition include $C_{12}A_7$, C_2S, C_3A, C_3S, and small amounts of free CaO and free MgO. Air quenching transforms $C_{12}A_7$ into an amorphous state and allows C_2S to form metastable β-C_2S crystal structures, improving the cementitious activity. In addition, the air quenching reduces the size of free MgO from 20–45 μm to 2–3.5 μm, which is about an order of magnitude reduction, thereby improving the volume stability. Furthermore, air quenching destroys the high-polymerization structure of the six-coordinated Al, transforming it into a low-polymerization state.

INTRODUCTION

The ladle arc refining furnace (LF) has been widely used as a major out-of-furnace refining technique due to its simple equipment, low investment cost, convenient operation, and good refining effect.[1,2] Ladle furnace slag (LFS) is the steel slag generated during the LF refining process.[3] According to statistics, producing 1 ton of refining molten steel generates 20–50 kg of refining slag,[4] which means that, at a rough estimation, China produces approximately 10 million tons of slag residue. However, at present, only a small amount of LFS can be recycled as metallurgical return materials (such as flux and slag material).[5,6] Most of the remaining LFS is disposed of and mixed with other wastes, such as converter steel slag and electric arc furnace oxidation slag, which have low re-utilization rates, leading to land occupation and environmental contamination.[7–9] Therefore, it is necessary to conduct a comprehensive study on the utilization of LFS.

The chemical and mineral composition of LFS is different from those of common industrial wastes, such as fly ash, blast furnace slag, converter steel slag, etc. The chemical composition of oxides mainly contains calcium oxide, alumina oxide, and other oxides (e.g., over-burned free MgO and free CaO). The minerals mainly include dodecacalcium heptaaluminate ($C_{12}A_7$), tricalcium aluminate (C_3A), and belite (C_2S), etc.[10–13] This is similar to the rapid setting cement sold in the United States, Japan, and South Korea.[14] Regulated set cement contains an important mineral, namely dodecacalcium heptaaluminate ($C_{12}A_7$) or calcium fluoroaluminate ($C_{11}A_7{\cdot}CaF_2$). This mineral has the characteristics of fast hydration and rapid setting, allowing concrete to achieve high early strength,[15–17] which is often used in urgent road repairs, construction in

(Received July 15, 2020; accepted October 23, 2020; published online November 16, 2020)

severe cold conditions, and construction of some military facilities.[18,19] It is similar to China's special types of cement, such as sulfoaluminate cement and aluminate cement.

The chemical and mineral composition mentioned above indicates that the LFS should have high hydration activity and hydraulicity, and have great utilization potential as a cementitious material. However, its application is limited at present. The reasons include the following.[1,20–22] First, similar to the converter steel slag, LFS formed by natural cooling of molten slag at 1560°C has dense and complete mineral crystals, large grains, and few defects. This dense crystalline $C_{12}A_7$ and C_3A has low reactivity, and the C_2S mineral formed by slow cooling is the γ-C_2S crystal form, which has almost no cementitious property, resulting in a slow hydration rate and undesirable cementitious properties. Second, LFS in the process of slow cooling produces free magnesium oxide (free MgO), and free calcium oxide (free CaO) and some complex and dense solid solutions, resulting in a slow hydration rate and volume expansion in later hydration stages, and affecting the volume stability of the material. Therefore, carrying out research on LFS with the focus on improving the mineral crystalline state and crystal type is beneficial to improve the cementitious properties of LFS, promoting its application in the construction materials industry.

Based on the analysis of phase transition of molten LFS during the cooling process, the temperature and cooling rate are the main factors affecting the crystallization state, crystal type, and structure. Therefore, this research adopted air-quenching treatment on high-temperature molten slag to optimize the crystalline state and crystal type of LFS, and investigated the characteristics of phase transition of the air-quenched LFS in the aspects of apparent morphology, mineral composition, phase micromorphology, and structure, etc. This helps to evaluate the effect of air quenching on the modification and optimization of the mineral phase of LFS, providing a theoretical foundation for the promotion of the application of LFS as a cementing material in the constructional materials industry.

MATERIALS AND METHODOLOGY

Raw Materials

The LFS used in this research was provided by Dalipal Special Type Equipment Manufacturing in Hebei, China. The chemical compositions of the LFS sample with and without air quenching is shown in Table I.

Experiments and Methodology

The Experiment of Air Quenching Treatment for LFS

The pretreatment includes the following steps. First, the raw bulk LFS was crushed by a laboratory jaw crusher, and ground to below 100 mesh with a laboratory ball mill to achieve uniformity in all parts of the sample, and finally the ground slag sample was oven-dried at 105°C.

The air-quenching treatment for LFS includes the following steps. The schematic of the process of the air-quenching system is shown in Fig. 1. The molten slag with a temperature of 1450–1550°C was stored in the slag bag. When the system operated, the slag was poured out from the slag bag, drained through the inclined channel, and granulated by the high-speed gas jet sprayed from a nozzle below. The produced grain slag then flew into the cooling cylinder where the grain slag exchanged heat with cooling air by convection in the air-quenching system and transferred heat to the cooling water by radiation in the external cooling water-quenching device. The holes in the external cylinder wall facilitated the discharge of cooled water and water vapor after accelerating the cooling rate. The consolidated grain slag was then transported to the storage tank through the conveyor belt below the cooling cylinder for subsequent processing.

Assessment Test for the Properties of Air-Quenched LFS

A test was conducted to assess the properties of the air-quenched LFS, consisting of apparent morphology, chemical composition, mineral composition, mineral phase micromorphology, and structure. The slow-cooled slag sample was taken as a reference group. The study then evaluated the optimization effects of air quenching on the physical and chemical properties and characteristics of the mineral phase of LFS.

(a) Analysis of chemical and mineral composition
An x-ray fluorescence analyzer was used to determine the oxide content in the LFS, with the target material of Rh, a voltage of 40 kV, and a current of 70 mA. An x-ray diffraction (XRD) analyzer was used to determine the mineral composition of the LFS with and without the air-quenching treatment, with the target material of CuK, a voltage of 40 kV, a current of 30 mA, a scanning rate of 15°/min, and s step size of 0.02°.

(b) Observation, analysis and identification of mineral micromorphology
First, epoxy resin was used to inlay the slag sample, and then 400, 600, 800, 1000, 1200, 1500, 3000, and 5000 mesh metallographic sandpapers were used to polish the slag sample. Next, test samples were obtained after being cleaned. Then, back-scattered scanning electron microscopy (BSEM) was used to observe the mineral phase, and the energy-dispersive x-ray (EDX) was used in conjunction to analyze the elemental composition of mineral phase, thus further identifying the type of mineral phase.

(c) Analysis of the coordination structure of silica

Table I. Chemical compositions of LFS with and without air quenching (%)

Types	CaO	SiO_2	Al_2O_3	Fe_2O_3	MgO	TiO_2	SO_3	MnO	Other
Slow-cooled LFS	57.09	16.18	18.46	0.65	3.66	0.44	1.09	0.08	2.35
Air-quenched LFS	57.58	16.44	18.91	0.61	3.21	0.45	1.07	0.09	1.64

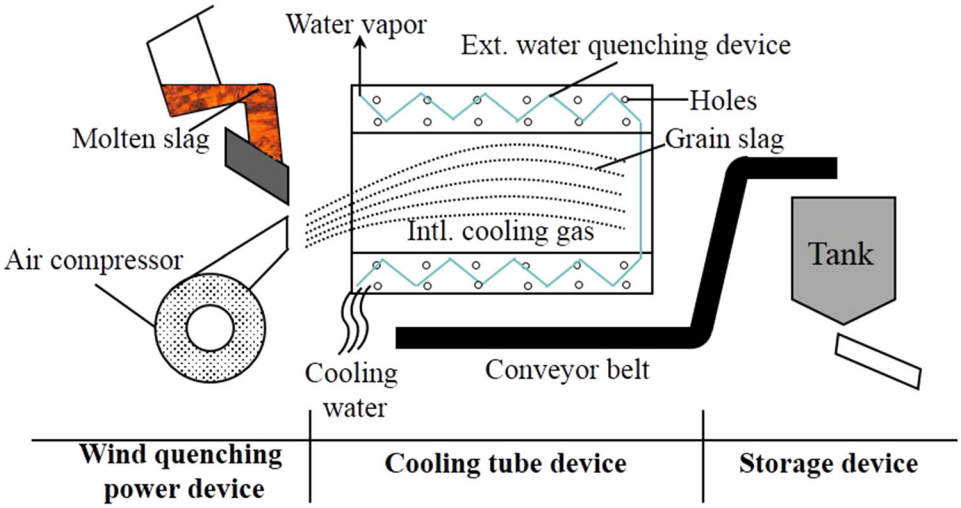

Fig. 1. Schematic of air-quenching treatment for LFS.

and aluminum

A BRUKER-AM 300 superconducting nuclear magnetic resonance (NMR) spectrometer produced the spectra of ^{29}Si and ^{27}Al NMR. ^{29}Si NMR used a zirconia rotor with a diameter of 7 mm and a length of 20 mm with a plastic cap. The resonance frequency was 59.62 MHz, the rotor operating frequency was 4000 rps, the repeat delay time was 2 s, the sampling time was 0.246 s, the pulse width was 45°, the spectrum width was 30 kHz, and data collection was 4000 points. ^{27}Al NMR used the same type of zirconia rotor, with the resonance frequency of 78.20 MHz, the rotor operating frequency of 4000 rps, the repetition delay time of 0.1 s, the sampling time of 40 ms, the pulse width of 45°, the spectrum width of 70 kHz, data collection of 4000 points, and accumulation times of 800, and the test was conducted at ambient temperature.

RESULTS AND DISCUSSION

The Apparent Morphology of the Air-Quenched LFS

The apparent morphology of LFS with and without air quenching is shown in Fig. 2. Compared to the irregular shape of slow-cooled LFS (cf. Fig. 2a), the air-quenched LFS has mainly gray-black spherical vitreous particles (cf. Fig. 2b), with the size varying from 3 mm to 10 mm for large grains and from 0.5 mm to 3 mm for small grains. At the same time, around 10% of the small-sized particles are lighter (relatively speaking versus gray–black particles) gray-white small particles which have smooth surfaces. Most of the spherical particles of the air-quenched LFS have a loose and porous structure and are easily ground.

The Analysis of Apparent Morphology of the Air-Quenched LFS

The results of SEM–EDX of LFS with and without air quenching treatment is shown in Fig. 3. In Fig. 3a, the selected upper, middle, and lower parts of the slow-cooled slag are shown to have a porous structure, a dense structure, and a loose structure, respectively. The results of the EDX analysis show that these three parts are composed of elements including Ca, Al, and Si, which form aluminate and silicate minerals. The silicon and magnesium content in the porous structure is relatively higher, and the content of aluminum is relatively lower. In Fig. 3b, the spherical particles of air-quenched LFS with two different colors (gray–black and gray–white) were analyzed. The results show that the gray–black particles are mainly composed of elements including Ca, Al, Si, and Mg. However, the Mg content in the gray-white particles is relatively high, and these particles are mainly composed of Ca, Al, and Mg. This result indicates that the air-quenching treatment may slightly enrich the Mg content in the LFS, allowing a small amount (about

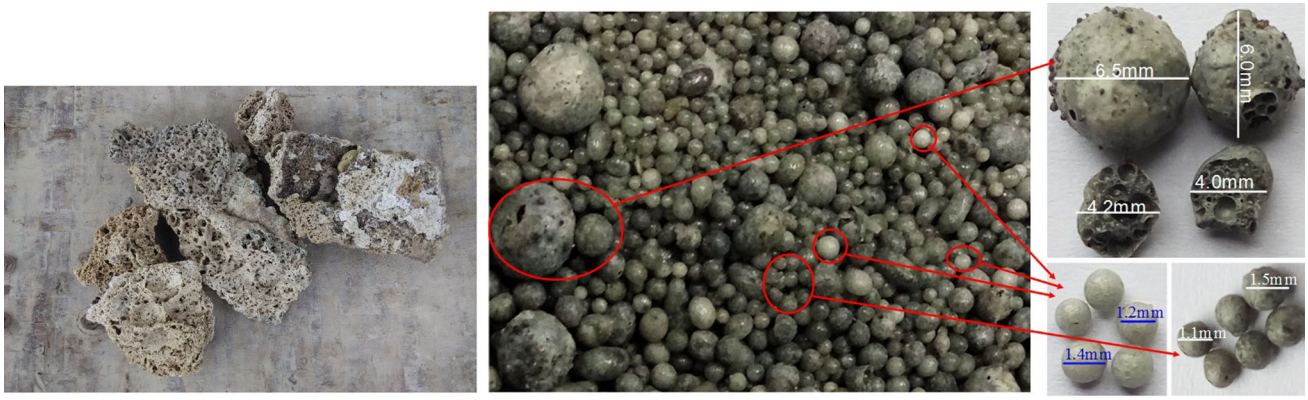

Fig. 2. Comparison of the apparent morphology of LFS with and without air quenching: (a) slow-cooled LFS, (b) air-quenched LFS.

10%) of gray-white spherical particles to form in the air-quenched LFS. This may mainly result from the difference between the melting point and the viscosity of the Mg compounds and that of the aluminate minerals.

Analysis of the Apparent Morphology of LFS with and Without the Treatment of Air Quenching

The BSEM–EDX results of LFS with and without air-quenching treatment are shown in Fig. 4. It can be seen from Fig. 4a that the mineral phase of the slow-cooled LFS in BSEM presents different apparent morphology and gray-scale levels of the mineral phase, mainly including black, dark gray, light gray, and white. The black minerals had quadrilaterals and other irregular shapes filled between dark gray and light gray minerals. The dark gray minerals exhibited partial polygons and other irregular shapes, interlaced with light gray minerals, which were continuously distributed in a matrix or stripes formation. The white minerals were inlaid in a round shape and stripes between other minerals, and their number was relatively small. The elemental compositions of the minerals with different gray-scales were obtained from the EDX analysis. The black minerals were mainly magnesium oxide minerals (i.e., free MgO). The dark gray minerals were mainly an aluminate mineral, $C_{12}A_7$, the light gray minerals were mainly a silicate mineral, C_2S, while the white minerals were mainly CaS.

However, compared to slow-cooled LFS, the morphology of the BSEM of the minerals in air-quenched LFS presented visible changes, as shown in Fig. 4b. There were many spherical holes in the air-quenched LFS, and the mineral phase also showed mainly four gray-scale levels: black, dark gray, light gray, and white. Light gray minerals were in a continuous distribution matrix, and the other minerals with three gray-scales were distributed or embedded in the matrix. Among them, the black minerals were distributed as irregular particles, the dark gray minerals were distributed in the shape of leaves or snowflakes, and a small amount of white minerals were distributed in the shape of round speckles. The elemental compositions of the minerals with different gray-scales were obtained from the EDX analysis. The light gray minerals were mainly aluminate minerals and silicate minerals (mixtures of amorphous $C_{12}A_7$ and C_2S), the black granular minerals were mainly magnesium oxide minerals, (i.e., free MgO), the dark gray leaf-like or snowflake-like minerals were mainly calcium oxide minerals, (i.e., free CaO), and the white minerals were mainly calcium sulfide (CaS) minerals.

The Impact of Air Quenching Treatment on the Free-MgO in LFS

The results presented above have illustrated that the air-quenching treatment has beneficial effects on the crystallization state and micromorphology of the mineral phase of LFS.[23] It is also necessary to investigate the effect of air quenching on free MgO in LFS because free MgO greatly influences the volume stability of cementitious materials. Figure 5 shows the morphology and size of free MgO in LFS with and without air quenching. As can be seen from Fig. 5a, free MgO in the slow-cooled LFS has four-sided rhombus and irregular shapes, and its dimensions are in the range of 20–45 μm. Compared with this, the free MgO particles in the air-quenched LFS have irregular shapes with smaller sizes, ranging from 2 μm to 3.5 μm (cf. Fig. 5b). This result indicates that the air-quenching treatment can significantly reduce the dimensions of free MgO in LFS, which is about an order of magnitude lower. This small size of free MgO has a higher hydration activity due to the low degree of dead burn or over-burn, which allows the free MgO to hydrate and dissolve in the early stage of the cementitious material hydration process, lowering the negative impact of the free MgO on the

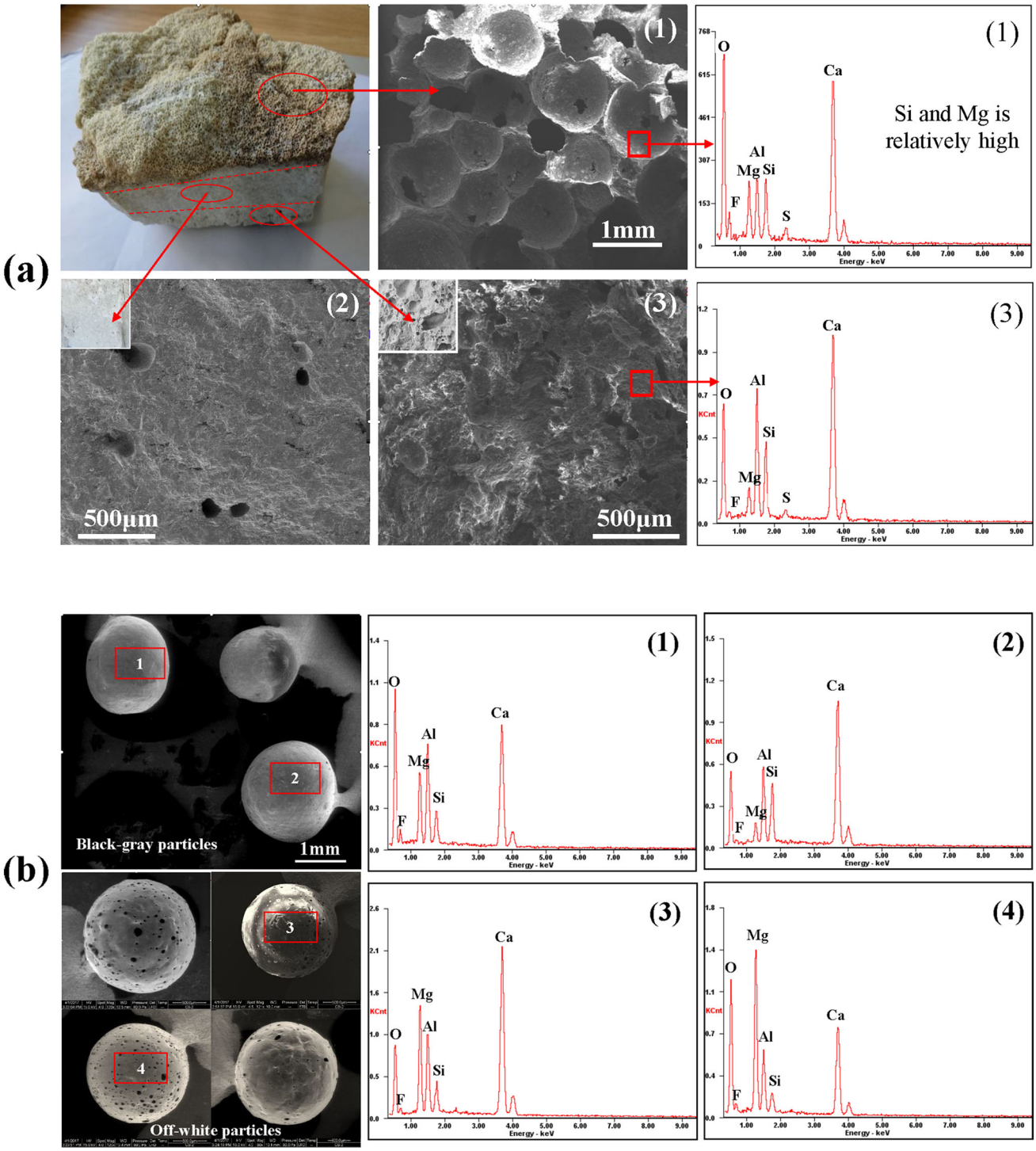

Fig. 3. A comparison analysis of scanning electron microscope and energy dispersive x-ray (SEM-EDX) results of LFS with and without air quenching: (a) typical areas of slow-cooled LFS, (b) different spherical particles of air-quenched LFS.

stability of cementitious materials.[10] Therefore, the air-quenching treatment contributes to improving the volume stability of LFS.

The Analysis of the Mineral Composition of Air-Quenched LFS

The XRD spectra of LFS with and without air-quenching treatment are shown in Fig. 6. The mineral composition remained unchanged, consisting mainly of $C_{12}A_7$, C_2S, C_3A, C_3S, and small amounts of free CaO, free MgO, and CaF. However, the crystalline state of

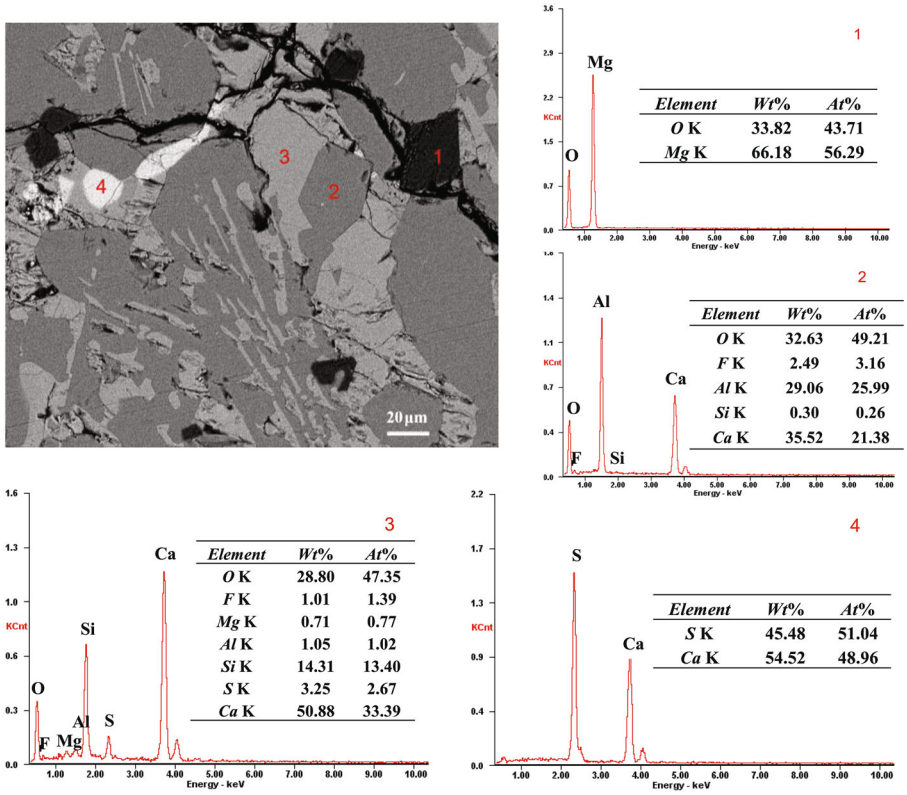

(a)

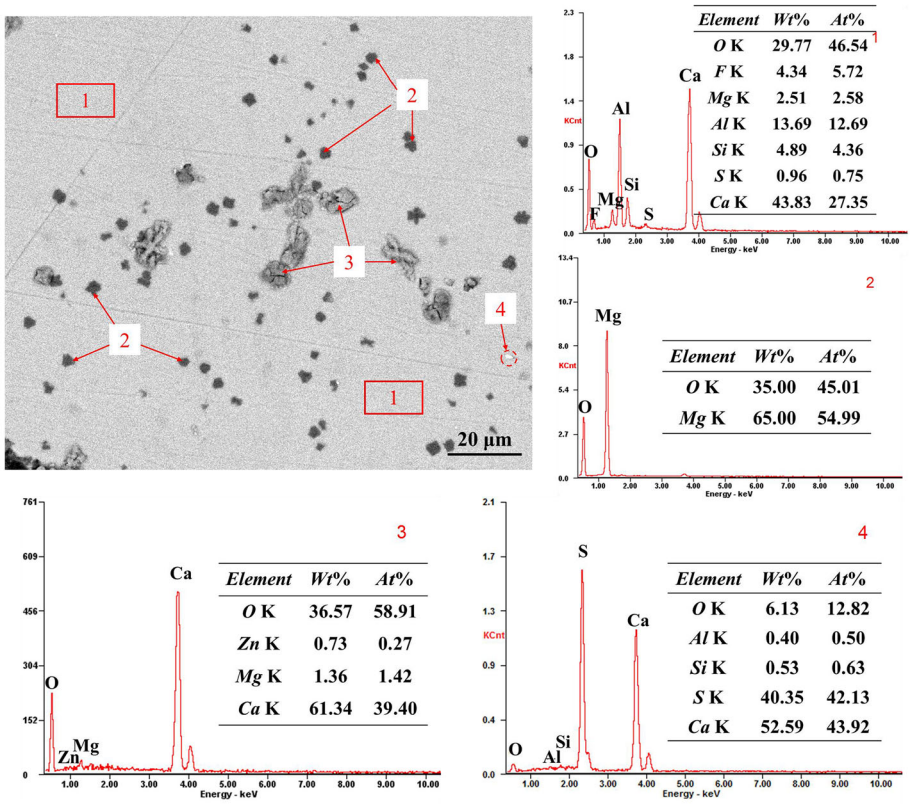

(b)

Fig. 4. A comparison analysis of back-scattered scanning electron microscopy and energy dispersive x-ray (BSEM-EDX) results of LFS with and without air-quenching treatment: (a) phases of slow-cooled LFS, (b) phases of air-quenched LFS.

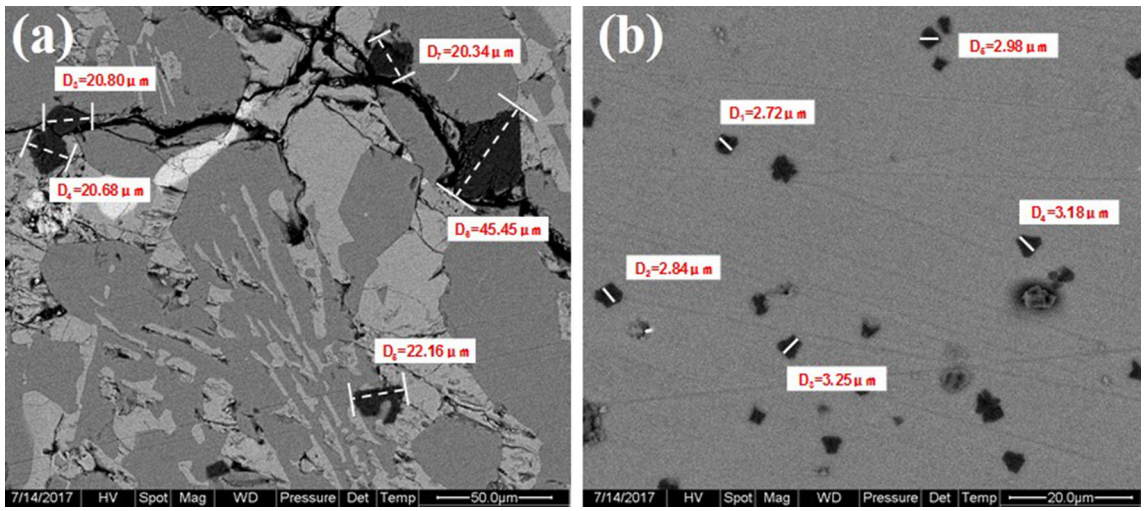

Fig. 5. A comparison of the morphology and size of free MgO with and without air-quenching treatment: (a) the state of free MgO in slow-cooled LFS, (b) the state of free MgO in air-quenched LFS. Here, D_i (i = 1,2,3…) represents the dimensions of free MgO in the LFS.

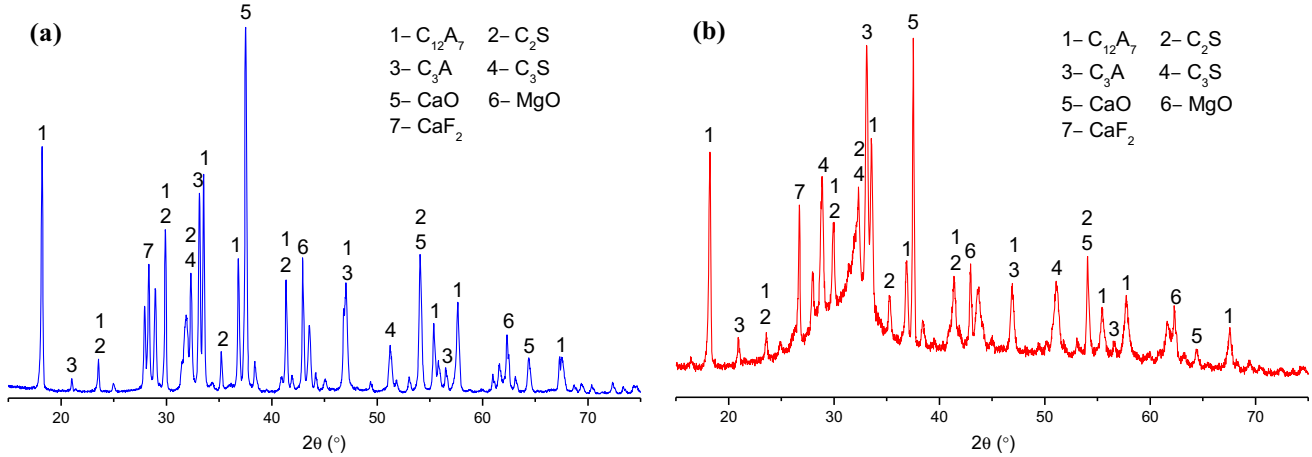

Fig. 6. A comparison of the XRD spectra of LFS with and without air-quenching treatment: (a) the mineral composition of slow-cooled LFS, (b) the mineral composition of air-quenched LFS.

the mineral phase had been subjected to great changes: the XRD spectrum of the slow-cooled LFS was a typical type of spectra of crystalline minerals (cf. Fig. 6a), indicating that its mineral phase was a crystalline phase, while the spectrum of the air-quenched LFS had an obvious amorphous "hump" feature (cf. Fig. 6b), indicating that the mineral phase contained a large number of amorphous mineral phases. Through further XRD analysis, it was confirmed that the $C_{12}A_7$ in the air-quenched LFS was mainly amorphous, and that the C_2S mineral was mainly in the β-C_2S crystal form. This shows that, after air quenching, the internal defects of the minerals of LFS will increase significantly, the dense crystalline state was destroyed, and amorphous materials appeared, allowing the C_2S mineral to be preserved in the metastable β-C_2S crystal form. The prevention of the crystal form transition from β-C_2S to γ-C_2S helps to improve the cementitious activity of LFS.[24]

Analysis of the Mineral Structure of LFS

LFS belongs to aluminosilicate minerals, and its mineral structure is crucial to the cementitious activity of the refining slag. Analysis and determination of its Al and Si coordination structure is an important way to characterize its mineral structure. NMR can determine both the ordered crystal structure and the disordered cementitious structure. The coordination structure of Al and Si can be determined by the chemical shift of ^{27}Al and ^{29}Si in the NMR spectrum for further study of mineral structures.[25,26] Al exists mainly in the form of four-coordinated [AlO_4] or six-coordinated [AlO_6] in aluminosilicate minerals, and sometimes has a structure of five-coordinated [AlO_5]. Si exists mainly in the form of silico-tetrahedral [SiO_4] structural units in aluminosilicate minerals. According to the bridge oxygen number connecting the silicon-oxygen tetrahedron [SiO_4] and other Si atoms, the type

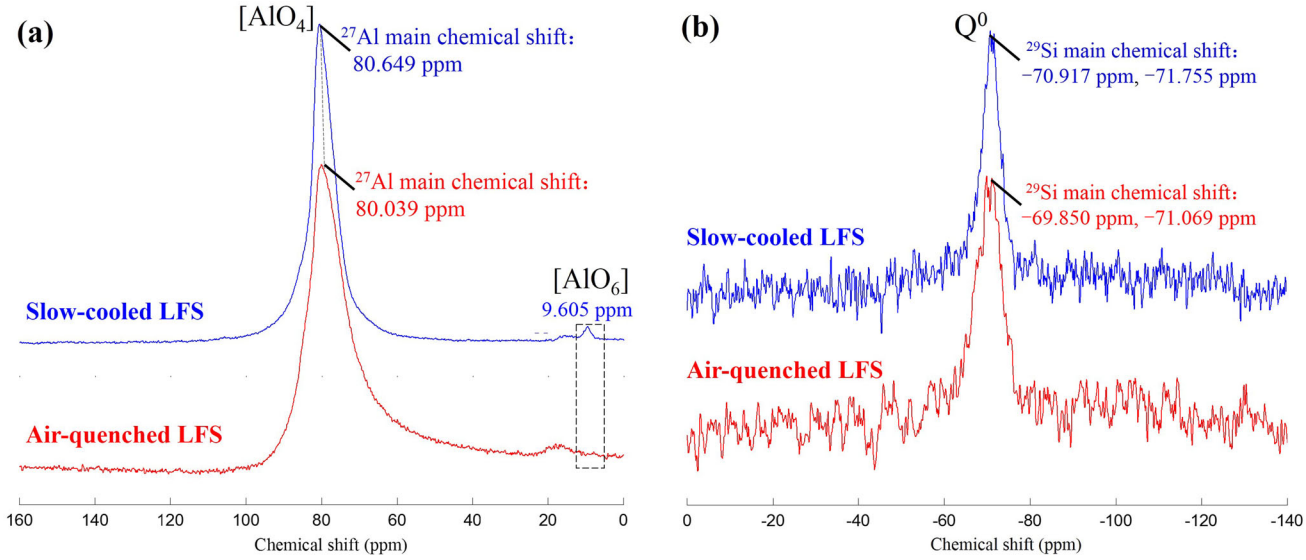

Fig. 7. A comparison of the NMR spectra of LFS with and without air-quenching treatment: (a) ^{27}Al-NMR spectrum of slow-cooled and air-quenched LFS, (b) ^{29}Si-NMR spectrum of slow-cooled and air-quenched LFS. Here, [AlO_4], [AlO_6] and Q^0 represent the form of four-coordinated Al, six-coordinated Al, and the coordination bridge oxygen number around Si in aluminosilicate minerals, respectively.

of ^{29}Si was divided into Q^0, Q^1, Q^2, Q^3, and Q^4 (where n in Q^n represents the coordination bridge oxygen number around Si).[27]

The NMR spectra of ^{27}Al and ^{29}Si of LFS are shown in Fig. 7. As shown in Fig. 7a, the major chemical shift of ^{27}Al in LFS was at 80.649 ppm, within the ranges of the four-coordinated structure of Al. On addition, a small peak at 9.605 ppm appeared in the spectrum, which was within the range of chemical shifts of the six-coordinated structures of Al. Therefore, slow-cooled LFS mainly existed as a four-coordinated [AlO_4] tetrahedral structure, with a small amount of a six-coordinated [AlO_6] octahedral structure. However, with the air-quenching treatment, the major chemical shift of ^{27}Al was at 80.039 ppm, and the small peak in the range of -10 to $+20$ ppm almost disappeared. Thus, the Al in the air-quenched LFS sample mainly existed as four-coordinated [AlO_4] tetrahedral structures, and the six-coordinated [AlO_6] octahedral structures had almost disappeared. Moreover, the range of the spectrum of ^{27}Al in LFS was widened, and the major peak was shifted rightward, indicating that air quenching has destroyed the high-polymerization structure of Al which is transitioned to low-polymerization. Amorphization of the Al-containing mineral phase (i.e. $C_{12}A_7$) dissolved in the silicate mineral (i.e. C_2S) occurred.[28]

From Fig. 7b, it can be seen that the main chemical shifts of ^{29}Si in slow-cooled and air-quenched LFS were closed, which are around -10 ppm and are in the range of the corresponding Q^0 structure. This indicates that Si in slow-cooled and air-quenched LFS existed as a structure of nesosilicate silicon tetrahedron [SiO_4], and air quenching had a minor impact on the coordination structure of Si in LFS. The LFS contained a large amount of network structure-changing Ca ions between [SiO_4] and [AlO_4], which increased the distortion of the system during melting and cooling. This will broaden the NMR absorption peak of LFS.

CONCLUSION

The following conclusions can be drawn from the experiment and analysis above:

(1) Air quenching changes the morphology of particles of LFS from irregular bulk shapes to spherical shapes with a porous structure, which is mainly composed of gray-black particles with Ca, Al, Si, and Mg elements, and a small amount of gray-white particles with Ca, Mg, and Al elements. The dimensions of the particles range from 0.5 mm to 10 mm.

(2) Air quenching significantly changes the micromorphology of the mineral phase of LFS: the slow-cooled LFS, exhibiting a clear and separated micromorphology, while the air-quenched LFS contains a matrix of continuously distributed aluminosilicate minerals, with a small amount of black granular free MgO, and snowflake-shaped free CaO, and white speckled CaS embedded in it.

(3) Air quenching significantly reduces the dimension of free MgO in LFS from 20–45 μm to 2–3.5 μm, which is approximately an order of magnitude lower, improving the volume stability of LFS.

(4) The mineral composition of LFS remains unchanged after air quenching, which includes mainly $C_{12}A_7$, C_2S, C_3A, and C_3S, and

small amounts of free CaO, free Mg, and CaF. Air quenching changes the crystalline state of $C_{12}A_7$ from crystalline to amorphous, allowing the C_2S minerals to be preserved in the metastable β-C_2S crystal form, improving the cementitious activity of LFS.

(5) The six-coordinated [AlO_6] octahedral structure of Al in air-quenched LFS mostly disappears, indicating that the air-quenching process destroyed the high-polymerization structure of the six-coordinated Al in LFS, making it transition to a low-polymerization state.

ACKNOWLEDGEMENTS

This work was financially supported by the National Natural Science Foundation of China (No. 51908568), the National Key Research and Development Program of China (No. 2019YFC1905104), the Natural Science Foundation of Guangdong Province (2019A1515011981), the Natural Science Foundation of Beijing, China (No. 2184118), and the State Key Laboratory open fund of Marine Resource Utilization in South China Sea (Hainan University) (201904).

CONFLICT OF INTEREST

On behalf of all authors, the corresponding author states that there is no conflict of interest.

REFERENCES

1. N.N. Lv, J.K. Yu, and C. Su, *China Metall.* 10, 1 (2011).
2. Q.F. Wu, Y.P. Bao, L. Lin, G.P. Xu, H.G. Cheng, Y. Huang, and C.P. Xin, *Steelmaking* 30, 50 (2014).
3. A.S.G. Vilaplana, V.J. Ferreira, A.M. López-Sabirón, A. Aranda-Usón, C. Lausín-González, C. Berganza-Conde, and G. Ferreira, *Constr. Build. Mater.* 94, 837 (2015).
4. H.Y. He, Z.Z. Zeng, J.G. Liu, B. Xu, and R.J. Cheng, *J. Wuhan Univ. Sci. Technol.* 33, 6 (2010).
5. F. Memoli, O. Brioni, and C. Mapelli, *Iron Steel Technol.* 4, 68 (2007).
6. Y.H. Kim, J.M. Yoo, D.S. Kim, J.H. Lim, and S.H. Yang, *J. Korean Inst. Resour. Recycl.* 22, 36 (2013).
7. M. Loncnar, H.A.V.D. Sloot, A. Mladenovič, M. Zupančič, L. Kobal, and P. Bukovec, *J. Hazard. Mater.* 317, 147 (2016).
8. V.Z. Serjun, A. Mladenovič, B. Mirtič, A. Meden, J. Ščančar, and R. Milačič, *Waste Manag* 43, 376 (2015).
9. B. Xu and Y. Yi, *Sci. Total Environ.* 705, 135854 (2020).
10. J.H. Zhao, Q. Liu, and K.Z. Fang, *Mater. Lett.* 128528, 280 (2020).
11. Z. Yildirim and M. Prezzi, *Adv. Civ. Eng.* 2011, 463638.1 (2011).
12. C.J. Shi, *Cement Concrete Res.* 32, 459 (2002).
13. H.M. Zhao and B. Xie, *Iron Steel Vanadium Titan.* 23, 53 (2002).
14. D. Knofel and J.F. Wang, *Cement Concrete Res.* 24, 801 (1994).
15. B.J. Hauspo, G.C. Hoff, and Y.W. Bi, *Low Temp. Archit. Technol.* 1, 57 (1979).
16. H. Uchikawa and S. Uchida, *Cement Concrete Res.* 2, 681 (1972).
17. A.J. Majumbar, B. Singh, and R.N. Edmonds, *Cement Concrete Res.* 19, 848 (1989).
18. H.G. Park, S.K. Sung, C.G. Park, and J.P. Won, *Cement Concrete Res.* 38, 379 (2008).
19. J.P. Won, U.J. Hwang, and S.J. Lee, *Cement Concrete Res.* 76, 121 (2015).
20. K. Pang, *Shanxi Archit.* 35, 164 (2009).
21. H.H. Liu, Z.Y. Liu, and W. Shao, *Steelmaking* 31, 73 (2015).
22. J.M. Montenegro-Cooper, M. Celemin-Matachana, J. Canizal, and J.J. González, *Constr. Build. Mater.* 203, 201 (2019).
23. M. Tossavainen, F. Engstrφm, Q. Yang, N. Menad, M.L. Larsson, and B. Bjorkman, *Waste Manag* 27, 1335 (2007).
24. C.J. Shi and S.F. Hu, *Cement Concrete Res.* 33, 1851 (2003).
25. J.M. Xiao and H.H. Fan, *J. Mater. Sci. Eng.* 34, 166 (2016).
26. Y.H. Fang, *J. Build. Mater.* 6, 54 (2003).
27. L. Chao, *Research on the Glass Phase Of Slag, High Calcium Fly Ash and Low Calcium Fly Ash and Their Hydration Mechanism*. Ph.D. Thesis (Tsinghua University, Beijing, 2011).
28. J.H. Li, H.H. Sun, and X.C. Tie, *J. Tsinghua Univ. (Sci. Technol.)* 46, 2015 (2006).